BIOCHEMISTRY
including biophysical chemistry & molecular biology
Article

Biochemistry **2009,** *48,* 10803–10809 10803
DOI: 10.1021/bi901301r

Interdomain Contacts in Flavocytochrome b_2, a Mutational Analysis

K. H. Diêp Lê,[‡] Alain Boussac,[§] Bettina Frangioni,[∥] Christophe Léger,[∥] and Florence Lederer*[,⊥]

[‡]*Laboratoire d'Enzymologie et Biochimie Structurales, CNRS UPR9063, 91198 Gif-sur-Yvette Cedex, France,* [§]*iBiTec-S, CNRS URA 2096, CEA Saclay, 91191 Gif-sur-Yvette Cedex, France,* [∥]*Unité de Bioénergétique et Ingéniérie des Protéines, UPR 9036, CNRS, IMM and Aix-Marseille Université, 31 Chemin Joseph Aiguier, 13402 Marseille Cedex 20, France, and* [⊥]*Laboratoire de Chimie Physique UMR 8000, Faculté des Sciences, Université Paris XI, 91405 Orsay Cedex, France*

Received July 28, 2009; Revised Manuscript Received October 9, 2009

ABSTRACT: Each flavocytochrome b_2 (L-lactate cytochrome *c* oxidoreductase) subunit consists of an N-terminal cytochrome domain and a C-terminal flavodehydrogenase (FDH) domain. In the enzyme crystal structure, only two heme domains are visible per enzyme tetramer, because of the mobility of the other two heme domains relative to the FDH domains. Evidence was subsequently provided that this mobility also exists in solution. Numerous kinetic studies showed that, during the catalytic cycle, electrons are transferred one by one from the reduced flavin to heme b_2 in the same subunit. In previous work, we provided evidence that a monoclonal antibody that abolishes flavin to heme electron transfer uses part of the interdomain interface for binding to its antigen, the native heme domain. In this work, we use a number of heme domain side chain substitutions in and around the interface to probe their effect on flavin to heme electron transfer. Using steady-state and pre-steady-state kinetics, as well as redox potential determinations and EPR measurements, we define several hydrophobic interactions and van der Waals contacts that are important for a catalytically competent docking of the heme domain onto the FDH domain. In addition, with several extremely slow mutant enzymes, we propose an isosbestic wavelength between oxidized and reduced heme for specifically following the kinetics of flavosemiquinone formation from two-electron reduced flavin.

Flavocytochrome b_2 (L-lactate cytochrome *c* oxidoreductase, EC 1.1.2.3) catalyzes L-lactate oxidation at the expense of cytochrome *c* in the mitochondrial intermembrane space in yeast and enables the latter to grow on lactate as the sole carbon source (*1*, *2*). Each subunit of the tetrameric enzyme comprises two domains. The first 99 residues encompass the heme binding site; residues 99−485 constitute the flavodehydrogenase (FDH)[1] domain, and residues 486−511 form contacts with the other subunits (*3*, *4*). Thus, the FDH domains constitute the enzyme tetrameric core, and the heme domains lie at its periphery. Each domain belongs to a different evolutionary family, the heme-binding one to the family of b_5-like cytochromes (*5*) and the FDH domain to the family of FMN-dependent L-2-hydroxy acid-oxidizing enzymes, with a $\beta_8\alpha_8$ fold (*6*, *7*).

In the crystal structure, the asymmetric unit presents electron density for two flavin-binding domains (a half-tetramer), but for only one heme-binding domain. This is due to the mobility of the domain around what is now called the hinge region, a segment of peptide chain of ∼10 residues (up to position 99) (*3*, *4*). The heme is located in a hydrophobic pocket, or crevice, with the propionates emerging at the surface. In the complete subunit, the opening of the heme crevice faces the flavin, at the C-terminal end of the $\beta_8\alpha_8$ barrel, with a distance of 9.6 Å between FMN N5 and the closest carbon atom of a porphyrin pyrrole ring, without any intervening side chain (*3*).

*To whom correspondence should be addressed: Laboratoire de Chimie Physique UMR 8000, Faculté des Sciences, Université Paris XI, 91405 Orsay Cedex, France. Telephone: 33 1 69 15 56 12. Fax: 33 1 69 15 61 88. E-mail: florence.lederer@lcp.u-psud.fr.

[1]Abbreviations: Fcb2, flavocytochrome b_2; FeCN, ferricyanide; FDH, flavodehydrogenase; Fl_{ox}, oxidized flavin; Fl_{red}, two-electron reduced flavin; Fl_{sq}, flavin semiquinone; SDM, site-directed mutagenesis; WT, wild type.

Scheme 1 shows the succession of electron transfer steps catalyzed by the enzyme, which has been the object of many studies over the years (*6*, *8*). Steady-state and stopped-flow studies, combined with deuterium isotope effect determinations and freeze-quench EPR spectroscopy, indicated that the lactate C2 hydrogen abstraction is rate-determining for flavin reduction and partially rate determining during turnover (*9*−*11*). Cytochrome *c* takes electrons only from heme b_2, while ferricyanide is reduced both by the heme and by the flavin semiquinone (Fl_{sq}) in the WT enzyme (*12*).

The heme domain mobility, first demonstrated in the crystal, raises a number of questions. First, are the contacts observed in the complete subunit in the crystal those required for efficient electron transfer between flavin and heme, and if so, which are the important ones? Second, is the heme domain mobility required or not for electron transfer between heme b_2 and cytochrome *c*? And finally, a question linked to the previous ones, what are the extent and frequency of the domain movements?

The first question has never been raised explicitly and may appear pointless, in view of the relative orientation of the prosthetic groups in the crystal, which appear close enough and in a proper orientation for allowing electron transfer between them. Nevertheless, the heme domain mobility may allow interactions other than those seen in the crystal. In solution, it is clear

Scheme 1: Fcb2 Catalytic Cycle

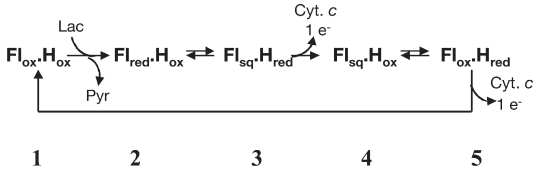

Published on Web 10/12/2009

that the interaction forces between the domains are not very strong, since separating the domains abolishes recognition and electron transfer between flavin and heme (*13*, *14*). Xia and Mathews (*3*) detailed an approximately equal number of interdomain nonpolar interactions and of hydrogen bonds and ionic interactions. Among the latter, there was only one salt bridge between a heme propionate and K296; in addition, some of the hydrogen bonds were actually contracted by water molecules bridging the domains. A few factors involved in functional docking have been analyzed by site-directed mutagenesis (SDM) and by manipulation of the sequence and length of the linker between the domains. For example, when active-site Y143, which forms a hydrogen bond with the second heme propionate, was mutated to a phenylalanine, the heme reduction rate was decreased (*15*, *16*). The importance of the structural integrity of the hinge region was demonstrated by the fact that either lengthening it or shortening it led to slower heme reduction (*17*−*19*).

In this work, we study the nature and importance for flavin to heme electron transfer of essentially nonpolar interdomain contacts observed in the crystal structure. We analyze the effect on the enzyme kinetics of 13 substitutions on 11 heme domain side chains that are located close to or within the interface between the FDH and heme domains. These substitutions had been previously engineered on the latter domain to map the epitope of a monoclonal antibody elicited against native Fcb2, which completely abolished heme reduction by the flavin (*20*, *21*). Parts of the results described in this work were presented in preliminary form previously (*22*, *23*).

MATERIALS AND METHODS

Site-directed mutagenesis and enzyme purification were conducted as described in ref *20*, as was the preparation of mutant heme domains by selective proteolysis of the corresponding mutant holoenzymes. Enzyme concentrations were expressed in terms of subunits, as monitored by the heme content after ascertaining that the heme to flavin ratio was 1/1 (ε^{ox}_{413} = 129.5 mM^{-1} cm^{-1}; ε^{red}_{423} = 183.0 mM^{-1} cm^{-1}).

Steady-state kinetics were performed at 30 °C in 0.1 M phosphate buffer and 1 mM EDTA (pH 7) with a Uvikon 930 double-beam spectrophotometer. The acceptors were 13 mM ferricyanide ($\varepsilon^{ox\text{-}red}_{420}$ = 1.04 mM^{-1} cm^{-1}) or Sigma horse heart cytochrome *c* at varying concentrations ($\varepsilon^{red\text{-}ox}_{550}$ = 20.5 mM^{-1} cm^{-1}). k_{cat} values are expressed as the number of moles of substrate consumed per mole of subunit per second. Pre-steady-state studies were conducted in the same buffer at 5 °C using an Applied Photophysics DX.17 MV stopped-flow spectrophotometer. Analysis of kinetic data was performed using the instrument software. FMN reduction rates [k_{red}^{F} (from **1** to **2**, Scheme 1)] were monitored by following absorbance changes at 438.1 nm (an isosbestic point between oxidized and reduced heme); heme b_2 reduction rates [k_{red}^{H} (steps **1**−**3**, Scheme 1)] were monitored at 557 nm (*9*). The semiquinone was followed at 350 nm, another heme isosbestic point (this work and ref *22*).

CW-EPR spectra were recorded using a standard ER 4102 (Bruker) X-band resonator with a Bruker ESP300 X-band spectrometer equipped with an Oxford Instruments cryostat (ESR 900). Determination of *g* values was done using an ER032M gaussmeter (Bruker). Spectra were recorded at liquid helium temperature. For these experiments, the enzyme buffer was exchanged with 0.1 M Hepes (pH 7). Indeed, it is well-known that during the freezing process the pH of a phosphate buffer-containing medium dramatically decreases (*24*, *25*). We checked that the activities were not altered by the buffer change relative to those determined in the usual phosphate buffer.

Redox potentials of most mutant heme domains were determined spectrophotometrically as described by Massey (*26*), using methylene blue as a mediator. Briefly, the reaction mixture contained 10 μM dye, 225 μM xanthine, 20 nM xanthine oxidase, and 4−5 μM heme domain, in 0.1 M phosphate buffer (pH 7), under anaerobiosis. The spectra were recorded with a HP8453 diode array spectrophotometer. For F39A Fcb2, it was difficult to find a spectrophotometrically suitable mediator. Its redox potential was therefore determined by redox titration with a combined Ag/AgCl electrode, at 24 °C, in 0.1 M K_2PO_4-HCl (pH 7) in an anaerobic cell flushed with argon. The reductant was sodium dithionite at an enzyme concentration of 14 μM. The equimolar mixture of mediators (1 μM) contained 1,2-naphthoquinone, phenazine methosulfate, phenazine ethosulfate, methylene blue, and 2-hydroxy-1,4-naphthoquinone, with redox potentials ranging from 145 to −145 mV.

RESULTS

Flavin Reduction and Reoxidation. Ferricyanide is commonly used as a cheap acceptor for assessing the Fcb2 turnover. As mentioned in the introductory section, with the WT enzyme, it cannot compete with the heme for electrons from fully reduced flavin, and its K_m^{app} is low, on the order of ≤0.1 mM. Nevertheless, it was shown with the heme-free enzyme (*12*), the isolated FDH domain (*13*, *27*), and enzymes carrying mutations that slow heme reduction (*28*) that ferricyanide can be reduced directly by the two-electron reduced flavin and not only by the semiquinone and the heme. In those cases, the ferricyanide K_m^{app} value is increased, as analyzed by Iwatsubo et al. (*12*). Therefore, we systematically used a high concentration of ferricyanide as the acceptor for the steady-state characterization of the mutated Fcb2 enzymes, as well as for the independent FDH domain, to ensure maximal flavin turnover even for those enzymes for which the heme reduction rate would be impaired. Flavin reduction in the absence of external acceptor was monitored in the stopped-flow apparatus at 438.1 nm, a heme isosbestic point (*9*). Typically, full enzyme reduction is biphasic (*9*, *29*). This was rationalized by the fact that lactate is a two-electron donor, while full enzyme reduction requires three electrons per subunit (six lactate molecules altogether per tetramer) (*9*, *11*). The rapid phase, with approximately two-thirds of the total amplitude, corresponds to the introduction into flavin of two electrons from a lactate molecule (four lactate per tetramer); these electrons are rapidly redistributed between flavin and heme within a subunit. The slow phase corresponds to an intersubunit electron reshuffling, to regenerate two Fl_{ox} molecules per tetramer for reduction by the last two required lactate molecules. This slow phase is irrelevant during turnover. In this work, we shall consider only the rapid phase. For flavin, k_{red}^{F} corresponds in principle to the formation of species **2** in Scheme 1.

Table 1 shows that, within error, the turnover rates of all mutant enzymes in the presence of ferricyanide appear to be identical to that of the WT enzyme. Similarly, the rate of pre-steady-state flavin reduction by saturating lactate does not appear to be modified by the substitutions in the heme domain, except perhaps for L65A and A67Q. With these latter mutant forms, the stopped-flow trace was actually triphasic at high

Table 1: Steady-State Flavin Turnover and Pre-Steady-State Flavin Reduction

enzyme	k_{cat}^{FeCN} (s^{-1})[a]	k_{red}^{F} (s^{-1})[b]
WT	214 ± 9	139 ± 11[c]
F39A	209 ± 6	140 ± 14
P44A	211 ± 12	153 ± 12
E63K	218 ± 18	140 ± 18
P64Q	207 ± 7	149 ± 6
P64R	212 ± 8	150 ± 19
L65A	196 ± 8	170 ± 8[c]
A67Q	190 ± 14	173 ± 13[c]
A67L	185 ± 12	161 ± 15
N69K	208 ± 12	157 ± 6
V70M	218 ± 10	150 ± 10
D72A	225 ± 10	152 ± 7
K73A	214 ± 15	144 ± 8
Y74F	223 ± 11	139 ± 3
FDH	259 ± 23[d]	170 ± 3

[a]Determined at 30 °C in the presence of 20 mM L-lactate and 13 mM ferricyanide. [b]Determined at 5 °C in the presence of 20 mM L-lactate. [c]Extrapolated to an infinite L-lactate concentration. [d]Taken from ref *27*. For other details, see Materials and Methods.

Table 2: Steady-State Cytochrome *c* Reduction and Pre-Steady-State Heme b_2 Reduction

enzyme	$k_{cat}^{cyt\ c}$ (s^{-1})[a]	$K_m^{cyt\ c}$ (μM)	k_{red}^{H} (s^{-1})[b]
WT	155 ± 15[c]	131 ± 2[c]	90 ± 5
F39A	39 ± 3	113 ± 22	22 ± 5
P44A	87 ± 2	20 ± 2	30 ± 3
E63K	139 ± 8	119 ± 7	73 ± 2
P64Q	168 ± 35	69 ± 22	66 ± 3
P64R	143 ± 15	61 ± 2	66 ± 2
L65A	62 ± 11	65 ± 5	17 ± 1
A67Q	63 ± 5	51 ± 12	11 ± 1
A67L	6 ± 1	32 ± 20	1 ± 1
N69K	108 ± 11	85 ± 4	78 ± 5
V70M	184 ± 21	92 ± 12	76 ± 2
D72A	171 ± 6	105 ± 13	87 ± 2
K73A	164 ± 7	97 ± 12	86 ± 1
Y74F	165 ± 5	109 ± 10	82 ± 3

[a]Determined at 30 °C in the presence of 20 mM L-lactate, extrapolated to an infinite cytochrome *c* concentration. [b]Determined at 5 °C, extrapolated to an infinite L-lactate concentration. [c]Taken from ref *28*. For other details, see Materials and Methods.

substrate concentrations, and this behavior will be further discussed below. On the whole, it appears that the FDH domain kinetic properties are not sensitive to the modifications in the heme domain. This is another manifestation of the apparent independence between the domains (see ref *6* for other examples).

Heme b_2 and Cytochrome c Reduction. Turnover in the presence of cytochrome *c* includes all the steps in Scheme 1, while k_{red}^{H} includes the steps leading to species **3** in Scheme 1 and therefore is not a microscopic rate constant either. The results of the kinetic measurements are presented in Table 2 as well as in Figure 1 for an easier comparison. It appears that for the F39A, P44A, L65A, and A67Q/L substitutions, flavin to heme electron transfer is seriously affected, since the flavin reduction rate (Table 1) is not modified. There is a weaker effect of the substitutions of P64 and E63. A drastic effect on the heme reduction rate is expected to induce a decrease in the turnover rate when cytochrome *c* is the electron acceptor; this is what is observed with the substitutions at positions 39, 44, 65, and 67.

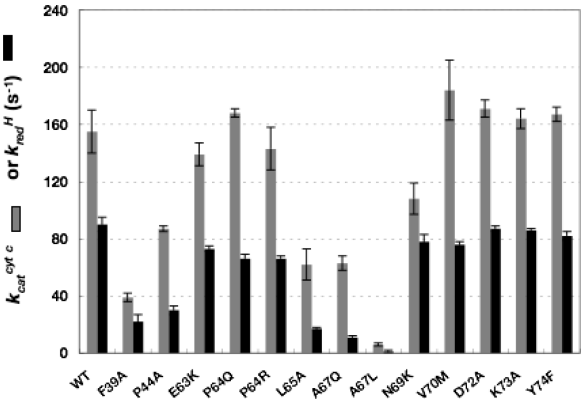

FIGURE 1: Steady-state cytochrome *c* reduction and pre-steady-state heme b_2 reduction. Gray bars depict data for cytochrome *c* reduction (k_{cat}) and black bars data for heme b_2 reduction (k_{red}^{H}). The rate constant values were taken from Table 2.

These results do not indicate if the substitutions also modify the interaction between the enzyme and cytochrome *c*. In contrast, it would appear that N69K Fcb2, with a nearly normal heme reduction rate, may have experienced a modification of the interaction with cytochrome *c*. The variations of the cytochrome *c* K_m values are not easy to interpret, due to the kinetic complexity of this parameter. One would expect an automatically lower value when a step prior to cytochrome *c* reduction has become more rate-limiting, which happens for the mutations at P44, P64, L65, and A67 (Table 2), but this effect should also be manifest for the mutation at F39 and is not observed. More work is required before we decide how the mutations specifically affect the interaction of Fcb2 with cytochrome *c*.

Redox Potentials of the Mutated Enzymes. The flavin to heme b_2 electron transfer rate may be modified because of thermodynamic factors and/or structural ones. Therefore, the redox potentials of the heme domains with mutations at positions 39, 44, 65, and 67 were determined. For the last three proteins, for which methylene blue proved to be a suitable indicator, the values were obtained using the spectrophotometric method proposed by Massey (*26*). For the F39A domain, however, we had to resort to a redox titration monitored by optical spectroscopy, as described in Materials and Methods. For the WT recombinant heme domain and for the one obtained by proteolysis, published values are −31 (*30*) and −28 mV (*31*), respectively, and in the holoenzyme −3 mV for the heme and −135 and −45 mV for the Fl_{red}/Fl_{sq} and Fl_{sq}/Fl_{ox} redox potentials, respectively (*32*). Table 3 gives the values determined in this work for the WT recombinant heme domain, and for the mutant domains obtained by proteolysis of the corresponding holoproteins. Clearly, the substitutions at positions 44, 65, and 67 do not significantly affect the heme redox potential. In contrast, for the F39A protein, the redox potential is lowered by ~55 mV, an effect that could be entirely responsible for the slower heme reduction rate in this mutant enzyme (Table 2 and Figure 1). This result is not unexpected. Indeed, the F39 phenyl ring covers part of the heme face on the side corresponding to H43, the first heme ligand. Its replacement with a methyl group would decrease the hydrophobicity of the heme environment and thus lower the redox potential (*33*). The structural comparison of the Fcb2 heme domain to its homologue bovine cytochrome b_5 shows an excellent superposition of the F39 phenyl ring with F35 (b_5) (*34*). Mutations of the latter residue to Y, H, and L lowered the cytochrome b_5 redox potential by 25−65 mV (*35*). Thus, altogether, it appears that the F39A

Table 3: Heme Redox Potentials

enzyme	E'_7 (mV), spectrophotometry	$E°$ (mV), electrochemistry
WT	3.3 ± 0.5	−6 ± 7
F39A		−60 ± 10
P44A	−4.7 ± 1.0	
L65A	6.3 ± 1.1	
A67Q	−3.3 ± 0.4	
A67L	−3.6 ± 0.2	

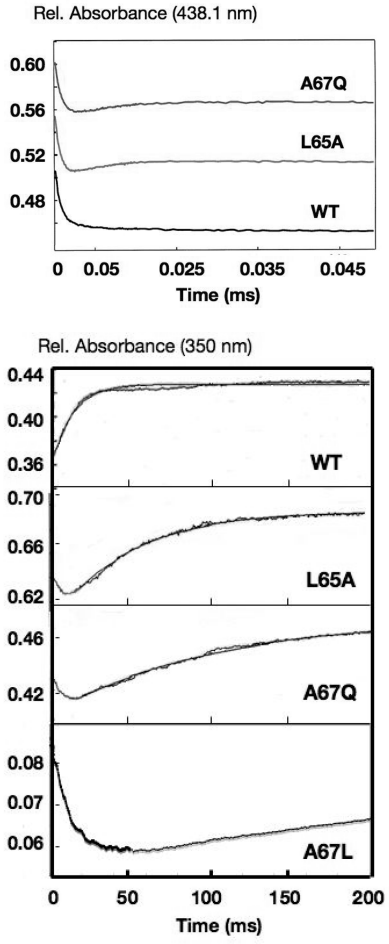

FIGURE 2: Stopped-flow monitoring of flavin reduction and semiquinone formation. The top panel shows flavin reduction at 438.1 nm (10 μM enzyme); the bottom panel shows semiquinone formation at 350 nm [20 μM enzyme, except for the A67L enzyme (13 μM)]. The lactate concentration was 20 mM in all cases. For experimental details, see Materials and Methods.

mutation is the only one for which there is a thermodynamic reason for the slower heme reduction rate. For the other mutant enzymes, there must be a structural origin, which will be discussed below.

Special Kinetic Behavior of the Enzymes Mutated at Positions 65 and 67. As mentioned above, the stopped-flow flavin reduction traces for the L65A and A67Q enzymes did not present the usual biphasic behavior at high substrate concentrations, as shown in Figure 2 (top) for the WT enzyme. They were actually triphasic; after ~20 ms, the absorbance at 438.1 nm increased somewhat and then started a very slow decrease (for ~100 s) to the level of fully reduced flavin. At low lactate concentrations, the traces presented the normal biphasic behavior. As Fl_{sq} has a higher absorbance at 438 nm than Fl_{red}, the absorbance increase was thought to arise from the appearance of Fl_{sq} (species **3** in Scheme 1). That this was actually the case was demonstrated in two different ways.

Table 4: Stopped-Flow Observation of Flavin Semiquinone Formation

wavelength	k_{red}^F (s^{-1})[a] at 438.1 nm	k_{sq}^F (s^{-1}) at 350 nm	k_{red}^H (s^{-1})[b] at 557 nm
WT	139 ± 11	106 ± 5	90 ± 5
L65A	170 ± 8	23 ± 1	17 ± 1
A67Q	173 ± 13	12 ± 1	11 ± 1
A67L	161 ± 15	1.1 ± 0.1	1 ± 1

[a]Taken from Table 1. [b]Taken from Table 2. All measurements were conducted at 5 °C. The values of k_{sq}^F were determined with 20 mM L-lactate.

First, with the availability of the spectra for all three redox states of the Fcb2 FMN in the recombinant FDH domain (*27*), it was possible to find another heme isosbestic point, at 350 nm, at which the semiquinone absorbs more than the two other flavin redox states. The stopped-flow traces at 350 nm are shown in Figure 2 (bottom). For the WT enzyme, formation of Fl_{sq} from Fl_{red} is already underway at the end of the dead time, while for the L65A and L67Q/L mutant enzymes, flavin reduction is still observable at that point. It can be seen in Table 4 that the rates of absorbance increase at 350 nm correspond, as expected, to the heme reduction rates determined at the α band maximum (557 nm).

Second, we resorted to EPR. Samples of WT, L65A, and A67Q Fcb2 were frozen at 198 K in a CO_2/ethanol bath and then in liquid helium, and the oxidized heme EPR signal was recorded at 15 K (not shown). The samples were then thawed, diluted with an equal volume of cold 40 mM L-lactate at the same temperature, and frozen within 1−2 s. With the WT enzyme, the heme EPR signal had completely disappeared, while some remained with the L65A enzyme and in particular with the A67Q sample. The solutions were thawed again, left for 2 min at room temperature, and frozen again, and the flavin spectra were recorded again. Figure 3 shows the semiquinone EPR spectra at the two freezing times, normalized to the intensity of the heme signal before enzyme reduction. It is clear that for the two mutant enzymes, the Fl_{sq} signal appears more slowly than for the WT enzyme and also disappears more slowly. These results support the interpretation of the triphasic stopped-flow traces observed at 438 nm.

DISCUSSION

A New Aspect of Intramolecular Electron Transfer Kinetics in Flavocytochrome b_2. As described above, the mutations at positions 65 and 67 turn out to have a drastic effect on flavin to heme electron transfer (Table 2 and Figure 1), among the largest effects ever observed with engineered Fcb2. The magnitude of this effect is materialized by the modification of the stopped-flow traces for flavin reduction at 438.1 nm at high substrate concentrations, from biphasic to triphasic (Figure 3), never previously reported for an Fcb2 derivative. This has led us to propose a new wavelength for specifically following the appearance and decay of Fl_{sq}; this wavelength corresponds to another isosbestic point for oxidized and reduced heme spectra, where Fl_{sq} has a higher absorbance than either Fl_{ox} or Fl_{red} (*27*). With the values for k_{red}^F (from **1** to **2**) and k_{red}^H (combined steps **1**−**3**) (Tables 1−3), using the simple kinetic scheme

1 → 2 → 3

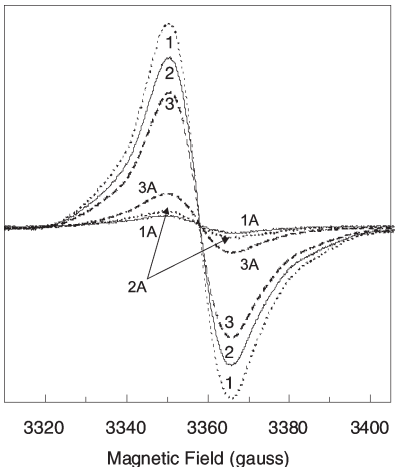

FIGURE 3: EPR spectra of the flavin semiquinone. Each enzyme in 0.1 M Hepes (pH 7) was mixed at 4 °C with an equal volume of 40 mM L-lactate (final enzyme concentration of ~150 μM) and immediately frozen at 198 K in a CO_2/ethanol bath and then in liquid helium [spectra 1 (WT), 2 (L65A), and 3 (A67Q)]. After the spectra had been recorded, the tubes were thawed, left for 2 min at 4 °C, and then frozen again, and new spectra were recorded (1A−3A). Instrument settings: temperature, 15 K; modulation amplitude, 2.8 G; microwave power, 100 μW; microwave frequency, 9.4 GHz; modulation frequency, 100 kHz.

one can evaluate the rate of Fl_{red} to heme electron transfer (from **2** to **3** above and in Scheme 1). Under our experimental conditions, it is on the order of 255 s^{-1} for the WT enzyme, and 19, 12, and 1 s^{-1} for L65A, A67Q, and A67L Fcb2, respectively. These values can be compared to those of k_{red}^{H} in Table 2. It is clear that for these mutated enzymes, flavin to heme electron transfer has become entirely rate-limiting in the overall turnover, in contrast to the partial rate limitation for the WT and the other mutated enzymes.

This calculation is, however, only approximate, not only for the fact that it neglects the slow phase contribution. Indeed, the results listed in Table 1 suggest that k_{red}^{F} is somewhat higher with L67A and A67Q/L Fcb2 than with the WT enzyme, but this higher value of k_{red}^{F} may not be an intrinsic property of these mutant enzymes. Since the Fl_{sq} absorbance at 438.1 nm is higher than that of Fl_{red}, albeit lower than that of Fl_{ox}, a sufficiently fast semiquinone formation will lead to a slower absorbance decrease at this wavelength than would happen for the single step of flavin reduction. This is the case for the WT enzyme and a number of mutant forms, but for enzymes such as L67A and A67Q/L Fcb2, there is less spectral interference from the slower electron transfer step from **2** to **3** (Scheme 1) with the flavin reduction step (**1** to **2**). Thus, the k_{red}^{F} values for these mutant enzymes are closer to if not identical with the intrinsic flavin reduction rate, and one should consider that the actual rate of flavin reduction by lactate is in most cases underestimated. This interpretation is in line with the fact that the flavin reduction rate we found in this work for the recombinant FDH domain is somewhat higher than that determined for the holoenzyme (Table 1).

Interdomain Contacts. None of the substitutions introduced into the Fcb2 heme domain affected reduction of flavin by lactate, indicating that the FDH domain functions in this respect in a manner independent of the other domain. This can be understood in light of the heme domain mobility disclosed by the crystal structure (*3*) and confirmed in solution (*36*). In contrast, flavin to heme electron transfer was affected by a number of substitutions. Among these, the replacement of the A67 methyl

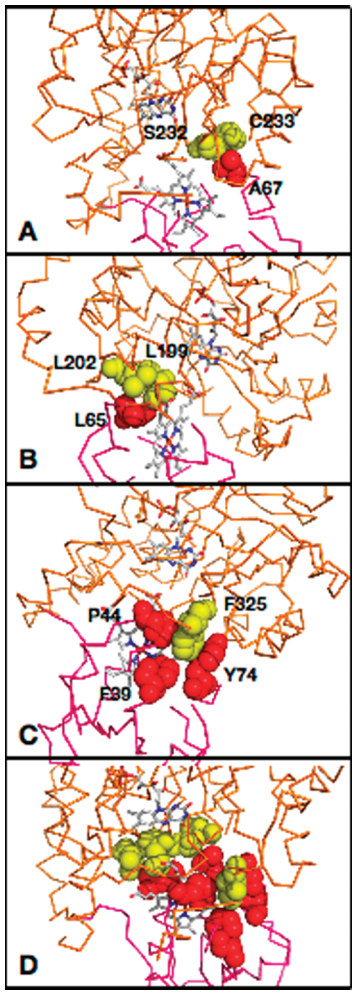

FIGURE 4: Important contacts between the flavin and the heme domains in WT Fcb2. The FDH domain CA trace is colored orange and that of the heme domain (up to residue 99) magenta: (A) contacts of A67 (red) with S232 and C233 (yellow), (B) contacts of L65 (red) with L199 and L202 (yellow), (C) hydrophobic pocket for F325 (yellow), made up by F39, P44, and Y74 (red), and (D) all the contacts shown in panels A−C. The figures were made using Pymol (*42*).

group with a bulky side chain was the one with the most drastic consequence (Figure 1 and Table 2). Inspection of the crystal structure shows that the A67 methyl group forms a van der Waals contact with Cys233 and its peptide oxygen and nitrogen atoms are engaged in hydrogen bonds with the peptide nitrogen and oxygen atoms of S232 (*3*) (Figure 4A). A bulky side chain at this position will prevent the heme domain from docking to the other domain in the same orientation and proximity as observed in the crystal. In contrast, replacing the L65 side chain with the methyl group of alanine removes a hydrophobic interaction of the side chain with those of L199 and L202 (Figure 4B). Interestingly, while the kinetic effect of the F39A mutation may be ascribed to the decreased redox potential of the mutated domain, it may also have in part a structural component. Indeed, as shown in Figure 4C, F39, P44, and Y74 form a hydrophobic pocket into which the phenyl ring of F325 is inserted. The importance of this interaction, both steric and hydrophobic, is supported by the effect of the P44A mutation which is also unfavorable for interdomain electron transfer. The aromatic group is still present in Y74F Fcb2; this rationalizes the absence of an effect of the mutation, which is also consistent with the fact that the phenol hydroxyl group does not appear to form any contacts (*3*). In the

subunit with the invisible heme domain, the orientation of the exposed F325 aromatic ring is slightly different; it would collide into P44 if one tried to dock the heme domain without modifiying the phenyl ring orientation. Finally, according to the crystal structure, P64 is close to the methylene groups of the K201 side chain. This interaction appears to be looser than those of L65 and A67, considering the moderate effect of its substitution with glutamine and arginine. All these interactions are listed in ref *3*, as well as a few others that we did not explore, namely, hydrophobic interactions involving P41 and P68 and hydrogen bonds involving N42 and the main chain of the second heme ligand, H66.

Figure 4D shows a global view of these interactions. Altogether, the interactions defined in this work underline the importance of steric complementarity and hydrophobic forces and confirm that the docking of the heme domain to the FDH domain observed in the crystal structure is competent for interdomain electron transfer. The strength of these interactions is altogether weak since, after physical separation by proteolysis (*14*) or genetic engineering (*13*), the domains do not recognize each other and do not exchange electrons. The docking is only possible when the peptide bond between residues 99 and 100 is present, acting as a leash that limits the space that can be sampled by the heme domain, before it encounters satisfactory contacts. This situation is probably due to the fact that few charged residues are present close to the interface, residues that could orient the domains with respect to each other, as proposed for the interactions of cytochrome *c* with its redox partners, in particular cytochrome b_5 (*37*−*40*). To the important interactions defined in this work must be added the hydrogen bond between the Y143 phenol group and a heme propionate (*3*, *15*, *16*). The Y143F mutation, under our working conditions, roughly doubles k_{red}^{F} and halves k_{red}^{H} relative to the WT values (*16*). In the crystal structure of Y143F Fcb2 at 2.9 Å resolution (Protein Data Bank entry 1LDC), the F143 phenyl ring can be superimposed onto the Y143 aromatic ring of the WT enzyme, with only the hydroxyl group missing (*41*). The authors pointed out a modified interaction between the domains, with four hydrogen bonds and eight hydrophobic interactions in the Y143F−pyruvate complex, compared with eight hydrogen bonds and eight hydrophobic interactions in the recombinant WT enzyme−sulfite complex. This interdomain hydrogen bond therefore also appears to participate in interdomain recognition.

The heme domain mobility may be due not only to rotations around the peptide bond between residues 99 and 100 demonstrated by the crystal structure but also to some flexibility of the so-called hinge region, which lies on the surface of the heme domain. Indeed, the crystal structure does not indicate many strong identifiable interactions of residues 90−99 with the body of the heme domain, apart from two hydrogen bonds between the peptide amido and carbonyl groups of D57 and the carbonyl and amido groups of L92 and C94, respectively. Furthermore, deletions of up to three residues in this segment still allowed electron transfer between flavin and heme, at a non-negligible rate [$k_{red}^{H} = 91\ s^{-1}$ with $k_{red}^{F} = 515\ s^{-1}$ compared to $k_{red}^{H} = 445\ s^{-1}$ and $k_{red}^{F} = 604\ s^{-1}$ for the WT enzyme at 25 °C (*18*)]. In view of these and previous results, one may even wonder if the experimentally determined heme reduction rate in the WT enzyme is not the statistical result of a series of more or less efficient electron transfers in suboptimal orientations of the prosthetic groups, formed during the heme domain movements. At present, there are no clues about how frequently the interactions observed in the crystal happen to be all formed in solution at the same time.

The enzymes studied in this work, which carried mutations in the heme domain, were generated for mapping the epitope of a monoclonal antibody against the holoenzyme that prevents electron transfer between the prosthetic groups (*20*). The results showed that the monoclonal antibody binds to an area overlapping in part the interdomain area. These mutant enzymes will also be of use for elucidating the cytochrome *c* binding area on Fcb2.

ACKNOWLEDGMENT

We are indebted to Dr. Bruno Guigliarelli for a critical reading of the manuscript.

REFERENCES

1. Daum, G., Böhni, P. C., and Schatz, G. (1982) Import of proteins into mitochondria. Cytochrome b_2 and cytochrome *c* peroxidase are located in the intermembrane space of yeast mitochondria. *J. Biol. Chem. 257*, 13028–13033.
2. Pajot, A. P., and Claisse, M. L. (1974) Utilization by yeast of D-lactate and L-lactate as sources of energy in the presence of antimycin. *Eur. J. Biochem. 49*, 275–285.
3. Xia, Z. X., and Mathews, F. S. (1990) Molecular structure of flavocytochrome b_2 at 2.4 Å resolution. *J. Mol. Biol. 212*, 837–863.
4. Cunane, L. M., Barton, J. D., Chen, Z. W., Welsh, F. E., Chapman, S. K., Reid, G. A., and Mathews, F. S. (2002) Crystallographic study of the recombinant flavin-binding domain of Baker's yeast flavocytochrome b_2: Comparison with the intact wild-type enzyme. *Biochemistry 41*, 4264–4272.
5. Lederer, F. (1994) The cytochrome b_5-fold: An adaptable module. *Biochimie 76*, 674–692.
6. Lederer, F. (1991) Flavocytochrome b_2. In Chemistry and Biochemistry of Flavoenzymes (Müller, F., Ed.) pp 153−242, CRC Press, Boca Raton, FL.
7. Lindqvist, Y., Brändén, C. I., Mathews, F. S., and Lederer, F. (1991) Spinach glycolate oxidase and yeast flavocytochrome b_2 are structurally homologous and evolutionarily related enzymes with distinctly different function and flavin mononucleotide binding. *J. Biol. Chem. 266*, 3198–3207.
8. Capeillère-Blandin, C. (1995) Flavocytochrome b_2 cytochrome *c* interactions: The electron transfer reaction revisited. *Biochimie 77*, 516–530.
9. Capeillère-Blandin, C., Bray, R. C., Iwatsubo, M., and Labeyrie, F. (1975) Flavocytochrome b_2: Kinetic studies by absorbance and electron-paramagnetic-resonance spectroscopy of electron distribution among prosthetic groups. *Eur. J. Biochem. 54*, 549–566.
10. Léger, C., Lederer, F., Guigliarelli, B., and Bertrand, P. (2006) Electron flow in multicenter enzymes: Theory, applications and consequences on the natural design of redox chains. *J. Am. Chem. Soc. 128*, 180–187.
11. Pompon, D., Iwatsubo, M., and Lederer, F. (1980) Flavocytochrome b_2 (baker's yeast). Deuterium isotope effect studied by rapid-kinetic methods as a probe for the mechanism of electron transfer. *Eur. J. Biochem. 104*, 479–488.
12. Iwatsubo, M., Mevel-Ninio, M., and Labeyrie, F. (1977) Rapid kinetic studies of partial reactions in the heme-free derivative of L-lactate cytochrome oxidoreductase (flavocytochrome b_2): The flavodehydrogenase function. *Biochemistry 16*, 3558–3566.
13. Balme, A., Brunt, C. E., Pallister, R., Chapman, S. K., and Reid, G. A. (1995) Isolation and characterization of the flavin-binding domain of flavocytochrome b_2, expressed independently in *Escherichia coli*. *Biochem. J. 309*, 601–605.
14. Gervais, M., and Tegoni, M. (1980) Spontaneous dissociation of a cytochrome core and a biglobular flavoprotein after mild trypsinolysis of the bifunctional *Saccharomyces cerevisiae* flavocytochrome b_2. *Eur. J. Biochem. 111*, 357–367.
15. Miles, C. S., Rouvière-Fourmy, N., Lederer, F., Mathews, F. S., Reid, G. A., Black, M. T., and Chapman, S. K. (1992) Tyr-143 facilitates interdomain electron transfer in flavocytochrome b_2. *Biochem. J. 285*, 187–192.
16. Rouvière, N., Mayer, M., Tegoni, M., Capeillère-Blandin, C., and Lederer, F. (1997) Molecular interpretation of inhibition by excess substrate in flavocytochrome b_2: A study with wild-type and Y143F mutant enzymes. *Biochemistry 36*, 7126–7135.

17. Sharp, R. E., Chapman, S. K., and Reid, G. A. (1996) Deletions in the interdomain hinge region of flavocytochrome b_2: Effects on intraprotein electron transfer. *Biochemistry 35*, 891–899.
18. Sharp, R. E., White, P., Chapman, S. K., and Reid, G. A. (1994) The role of the interdomain hinge of flavocytochrome b_2 in intra- and inter-protein electron transfer. *Biochemistry 33*, 5115–5120.
19. White, P., Manson, F. D. C., Brunt, C. E., Chapman, S. K., and Reid, G. A. (1993) The importance of the interdomain hinge in intramolecular electron transfer in flavocytochrome b_2. *Biochem. J. 291*, 89–94.
20. Lê, K. H. D., Mayer, M., and Lederer, F. (2003) Epitope mapping for the monoclonal antibody that inhibits intramolecular electron transfer in flavocytochrome b_2. *Biochem. J. 373*, 115–123.
21. Miles, C. S., Lederer, F., and Lê, K. H. D. (1998) Probing intramolecular electron transfer within flavocytochrome b_2 with a monoclonal antibody. *Biochemistry 37*, 3440–3448.
22. Lê, K. H. D., Boussac, A., and Lederer, F. (2005) in Flavins and Flavoproteins 2005 (Nishino, T., Miura, R., Tanokura, M., and Fukui, K., Eds.) pp 443−448, ArchiTect Inc., Tokyo.
23. Lê, K. H. D., and Lederer, F. (2002) in Flavins and Flavoproteins 2002 (Chapman, C., Perham, R., and Scrutton, N., Eds.) pp 597−603, Weber, R., Agency for Scientific Publications, Cambridge, U.K.
24. Kerfled, C. A., Yoshida, S., Tran, K. T., Yeates, T. O., Cascio, D., Bottin, H., Berthomieu, C., Sugiura, M., and Boussac, A. (2003) The 1.6 Å resolution structure of Fe-superoxide dismutase from the thermophilic cyanobacterium *Thermocynechococcus elongatus*. *J. Biol. Inorg. Chem. 8*, 707–714.
25. van den Berg, L., and Rose, D. (1959) Effect of freezing on the pH and composition of sodium and potassium phosphate solutions; the reciprocal system KH2PO4-Na2-HPO4-H2O. *Arch. Biochem. Biophys. 81*, 319–329.
26. Massey, V. (1991) A simple method for the determination of redox potentials. In *Flavins and flavoproteins 1990* (Curti, B., Ronchi, S., and Zanetti, G., Eds.) pp 59−66, Walter de Gruyter, Berlin.
27. Cénas, N., Lê, K. H. D., Terrier, M., and Lederer, F. (2007) Potentiometric and further kinetic characterization of the flavin-binding domain of *Saccharomyces cerevisiae* flavocytochrome b_2. Inhibition by anion binding in the the active site. *Biochemistry 46*, 4661–4670.
28. Rouvière-Fourmy, N., Capeillère-Blandin, C., and Lederer, F. (1994) Role of tyrosine 143 in lactate dehydrogenation by flavocytochrome b_2. Primary kinetic isotope effect studies with a phenylalanine mutant. *Biochemistry 33*, 798–806.
29. Ogura, Y., and Nakamura, T. (1966) Kinetic studies on the oxidation and reduction of the protoheme moiety of yeast L-(+)-lactate dehydrogenase. *J. Biochem. 60*, 77–86.
30. Brunt, C. E., Cox, M. C., Thurgood, A. G. P., Moore, G. R., Reid, G. A., and Chapman, S. K. (1992) Isolation and characterization of the cytochrome domain of flavocytochrome b_2 expressed independently in *Escherichia coli*. *Biochem. J. 283*, 87–90.
31. Labeyrie, F., Groudinsky, O., Jacquot-Armand, Y., and Naslin, L. (1966) Propriétés d'un noyau cytochromique b_2 résultant d'une protéolyse de la L-lactate: Cytochrome *c* oxydoréductase de la levure. *Biochim. Biophys. Acta 128*, 492–503.
32. Tegoni, M., Silvestrini, M. C., Guigliarelli, B., Asso, M., Brunori, M., and Bertrand, P. (1998) Temperature-jump and potentiometric studies on recombinant wild type and Y143F and Y254F mutants of *Saccharomyces cerevisiae* flavocytochrome b_2: Role of the driving force in intramolecular electron transfer kinetics. *Biochemistry 37*, 12761–12771.
33. Kassner, R. J. (1973) A theoretical model for the effect of local nonpolar heme environments on the redox potentials in cytochromes. *J. Am. Chem. Soc. 95*, 2674–2677.
34. Durley, R. C. E., and Mathews, F. S. (1996) Refinement and structural analysis of bovine cytochrome b_5 at 1.5 Å resolution. *Acta Crystallogr. D52*, 65–76.
35. Yao, P., Xie, Y., Wang, Y. H., Sun, Y. L., Huang, Z. X., Xiao, G. T., and Wang, S. D. (1997) Importance of a conserved phenylalanine-35 of cytochrome b_5 to the protein's stability and redox potential. *Protein Eng. 10*, 575–581.
36. Labeyrie, F., Beloeil, J. C., and Thomas, M. A. (1988) Evidence by NMR for mobility of the cytochrome domain within flavocytochrome b_2. *Biochim. Biophys. Acta 953*, 134–141.
37. Mauk, A. G., Mauk, M. R., Moore, G. R., and Northrup, S. H. (1995) Experimental and theoretical analysis of the interaction between cytochrome *c* and cytochrome b_5. *J. Bioenerg. Biomembr. 27*, 311–330.
38. Ren, Y., Wang, W. H., Wang, Y. H., Case, M., Qian, W., McLendon, G., and Huang, Z. X. (2004) Mapping the electron transfer interface between cytochrome b_5 and cytochrome *c*. *Biochemistry 43*, 3527–3536.
39. Salemme, F. R. (1976) An hypothetical structure for an intermolecular electron transfer complex of cytochromes *c* and cytochrome b_5. *J. Mol. Biol. 102*, 563–568.
40. Deep, S., Im, S. C., Zuiderweg, E. R. P., and Waskell, L. (2005) Characterization and calculation of a cytochrome *c*-cytochrome b_5 complex using NMR data. *Biochemistry 44*, 10654–10668.
41. Tegoni, M., Begotti, S., and Cambillau, C. (1995) X-ray structure of two complexes of the Y143F flavocytochrome b_2 mutant crystallized in the presence of lactate or phenyllactate. *Biochemistry 34*, 9840–9850.
42. DeLano, W. L. (2002) The PyMOL Molecular Graphics System, DeLano Scientific, San Carlos, CA.